

Factors Affecting Properties of Polymer Grouted Sands

Costas A. Anagnostopoulos* and Vasilios Aggelidis

Department of Environmental Engineering, International Hellenic University, Sindos, 57400 Thessaloniki, Greece; aggelidbill@gmail.com

* Correspondence: kanagnos@cie.teithe.gr; Tel.: +30-2310-013872

Abstract: The aim of this research was to undertake laboratory testing to investigate the beneficial effects of epoxy resin grouts on the physical and mechanical properties of sands with a wide range of granulometric characteristics. Six sands of different particle size and uniformity coefficients were grouted using epoxy resin solutions with three ratios of epoxy resin to water (3.0, 2.0 and 1.5). A set of unconfined compressive strength tests were conducted on the grouted samples at different curing periods and a set of long-term unconfined compressive creep tests in dry and wet conditions after 180 days of curing were also carried out in order to evaluate the development of the mechanical properties of the sands, as well as the impact of water on them. The findings of the investigation showed that epoxy resin resulted in appreciable strength values in the specimens, especially those of fine sands or well graded sands, grouted with the different epoxy resin grouts. Whilst the higher compressive strength and elastic modulus values at the age of 180 days were obtained for the finer sand, which ranged from 2.6 to 5.6 MPa and 216 to 430 MPa, respectively, the lower compressive strength and elastic modulus values were attained for the coarser sand with low values of the coefficient of uniformity, which varied from 0.68 to 2.2 MPa and 75 to 185 MPa, respectively. Moreover, all grouted sands showed stable long-term creep behaviour, with high values of the creep limit ranging from 67.5 to 80% of compressive strength. The presence of water had a negative marginal effect in the majority of the grouted specimens. In terms of physical properties, the permeability and porosity were estimated. The permeability of fine sands or well graded sands was decreased by two to four orders of magnitude. Using laboratory results and regression analysis, three mathematical equations were developed that relate each of the dependent variables of compressive strength, elastic modulus and coefficient of permeability to particular explanatory variables.



Citation: Anagnostopoulos, C.A.; Aggelidis, V. Factors Affecting Properties of Polymer Grouted Sands. *CivilEng* **2024**, *5*, 65–88. <https://doi.org/10.3390/civileng5010004>

Academic Editor: Angelo Luongo

Received: 23 November 2023

Revised: 2 January 2024

Accepted: 9 January 2024

Published: 11 January 2024



Copyright: © 2024 by the authors. Licensee MDPI, Basel, Switzerland. This article is an open access article distributed under the terms and conditions of the Creative Commons Attribution (CC BY) license (<https://creativecommons.org/licenses/by/4.0/>).

Keywords: epoxy resin; grout; creep; strength; permeability; porosity; regression analysis

1. Introduction

In the permeation grouting method, the grouting material is injected into the voids of soil at a constant rate, without changing the arrangement of soil particles, in order to improve its physical and mechanical properties by binding the soil particles together. In the case of clean sands and gravels with a coefficient of permeability higher than 10^{-5} m/s [1], injectable cement slurries are of great use in many construction domains. They provide satisfactory solutions for improving ‘problematic’ soils, since they can effectively penetrate through a large area of the soil mass. However, in soils with very low permeability, such as fine sands, the propagation of cementitious grouts is highly restricted, or even impossible, if a very fine cement is utilised. Because of this, permeation grouting in such soils requires the use of chemical solutions only.

For the purpose of chemical grouting, a large number of researchers have investigated the efficacy of using different types of polymer grouts for soil improvement, including polyurethane liquid [2], water soluble latex [3], acrylic resin and methylmethacrylate [4], dilute colloidal silica [5], polyvinyl acetate [6] and polyester [7]. The use of the aforementioned materials primarily aims at sealing the effective pore space of soils, resulting in an appreciable reduction in permeability, whereas the strength of the grouted soil tends to

be secondary, since it is limited to low levels. For example, the unconfined compressive strength (UCS) of a silty sand grouted with acrylate or acrylamide grouts is in the order of 0.8 MPa [8]. For sands grouted with colloidal silica, the UCS is in the range of 0.3 to 0.5 MPa [9,10] or even lower [11]. Therefore, it is crucial to aid in the research of new chemical grouts that could yield a more appreciable improvement in the strength of the solidified ground and that could be used effectively in many geotechnical and foundation applications, such as the increase of bearing capacity or the reduction of the settlement of fine grained compressible soils for building foundations, the stabilisation of deep excavations, slope stability, tunnel support, curtain grouting under dams and water control in tunnels, trenches, mine shafts and other excavations. More recently, some investigators have suggested two-component water-soluble epoxy resin emulsions, which are among the most widely applied polymeric compounds in many construction and building restoration projects [12–15], as grouting agents that can significantly improve the properties of weak soils. Despite the importance of this innovative material, limited published data are available to provide a comprehensive review regarding its applicability. Anagnostopoulos and Hadjispyrou [16], from experiments on poorly graded siliceous sand, stated that the finer the sand, the greater the improvement in its physical and mechanical properties induced by epoxy resin (ER) grouts. However, satisfactory strength was not observed (compressive strength of 1 MPa and elastic modulus of 60 MPa). This observation is in contradiction with the results published by Khanbashi and Abdala [17]. They performed UCS strength tests on poorly graded sand mixed with resin polymer. These tests showed a significantly higher compressive strength and elastic modulus of 10 MPa and 1,200 MPa, respectively. Anagnostopoulos et al. [18,19] evaluated the mechanical properties of a medium siliceous sand prepared in two different relative densities D_r of 50 and 90% and grouted with different ER compositions. They demonstrated that the improvement of strength parameters depends directly on D_r and the epoxy resin to water (ER/W) ratio. Additionally, Anagnostopoulos [20] performed strength tests on mixtures of ER and a clayey soil. The resultant compressive strength and elastic modulus values ranged from 0.88 to 2.34 MPa and 56 to 260 MPa, respectively. Similar results were attained by Ghasemzadeh et al. [21]. On the contrary, Halabian et al. [22] conducted tests on uniformly graded silty sand grouted with ER and found much higher strength, compressive strength and elastic modulus values that varied from 3 to 4.5 MPa and 200 to 330 MPa, respectively. As can be seen, the data available to date for the physical and mechanical properties of soils grouted with ER are still scarce and, in some cases, contradictory. Consequently, a general rule cannot be deduced regarding the efficacy of such materials for ground improvement purposes, or which are the main parameters that influence the strength of the stabilised soil. This inconsistency between the published results may be due to the different combinations of soil composition, particle size, index, relative density and grout proportion, which probably affected the laboratory findings. For these reasons, there is still a need to broaden the research in order to highlight the effect of some key factors (mainly the mean grain size d_{50} , the uniformity coefficient c_u and the type of soil) on the properties of the grouted soil, as well as the impact of the moisture conditions on the mechanical behaviour of grouted soils under static loading.

In order to gain knowledge about the effectiveness of epoxy resin (ER) grouts in soil improvement, and to address to some extent the research gap, an extensive laboratory study was performed to examine the relationships between the aforementioned parameters and some physical (porosity, permeability) and mechanical (compressive strength, elastic modulus, creep behaviour) properties of fine- to medium-grained sands grouted with epoxy resin. The grouts were produced using various epoxy resin to water (ER/W) ratios.

2. Materials

The epoxy resin employed in this study is a two-component water soluble commercial product widely distributed in Greece. Bisphenol A (epichlorhydrin) is the epoxy resin (part A), with an average molecular weight of approximately 700, and aliphatic gly-

cidylether (part B) is the reactant agent for the polymerisation of the resin [16,18–20,23]. According to the manufacturer, the optimal mixture ratio (by weight) of the two parts is A:B = 3.

Two types of soil, calcareous and siliceous sand were collected from river deposits and utilised for the injection experiments. From calcareous sand, six different sand gradations were chosen with particle sizes ranging from 1.19 to 0.42 mm (denoted as S₁), 0.42 to 0.149 mm (S₂), 0.149 to 0.074 mm (S₃), 1.19 to 0.074 mm (S₄), 2.38 to 0.074 mm (S₅) and 2.38 to 1.19 mm (S₆). Their gradation curves are depicted in Figure 1 and their index properties are summarised in Table 1. For the siliceous sand, a particle size distribution in the same range as the S₁ sand was chosen, as well as similar index properties.

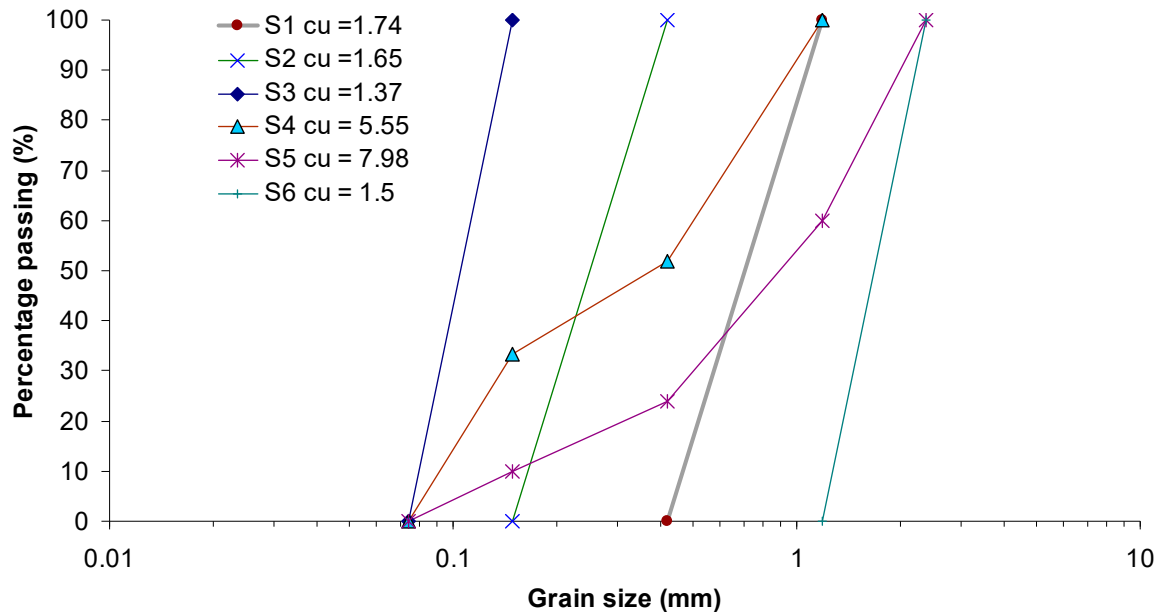


Figure 1. Gradation curves of the used sands.

Table 1. Index properties of the sands.

	S ₁	S ₂	S ₃	S ₄	S ₅	S ₆
D ₆₀ (mm)	0.8	0.28	0.11	0.5	1.19	1.85
D ₅₀ (mm)	0.67	0.2	0.097	0.33	0.8	2
D ₃₀ (mm)	0.57	0.21	0.091	0.15	0.39	1.31
D ₁₀ (mm)	0.46	0.17	0.08	0.09	0.149	1.22
Coefficient of uniformity, C _u	1.74	1.65	1.37	5.55	7.98	1.52
Coefficient of curvature, C _c	0.88	0.92	0.94	0.5	0.86	0.76
Specific gravity, G _s	2.66	2.66	2.66	2.66	2.66	2.66
Maximum void ratio, e _{max}	0.78	0.87	0.96	0.64	0.564	0.88
Minimum dry unit weight, γ _{dmin} (kN/m ³)	14.9	14.2	13.5	16.25	17	14.15
Minimum void ratio, e _{min}	0.62	0.61	0.64	0.47	0.364	0.576
Maximum dry unit weight, γ _{dmax} (kN/m ³)	16.4	16.5	16.2	18.1	19.5	16.87

3. Laboratory Procedure

Grouts with ER/W ratios of 1.5, 2.0 and 3.0 (by weight) were prepared for the grouting experiments. The sand columns were grouted using an arrangement constructed according to the laboratory system suggested in ASTM D 4320-09 [24]. A mixing tank with a high-speed agitator, an air-operated diaphragm pump, pressure regulator, pressure meters, flow meter and plastic cylindrical moulds (with an internal diameter of 5.5 cm and 150 cm high), as well as the relevant connections, constituted the experimental set-up for the laboratory assessment of the chemical grouting operations (Figure 2). In order to keep the grouted specimens intact upon removal from the moulds, after the end of injection, the inner surface

of the mould was lubricated before pouring the sand. Special precautions were taken for the filling process of the columns with the gravel material, to ensure the uniformity of the specimens and the desired relative density D_r of 50%. The exact weight of sand required to fill the mould was calculated and this quantity was poured into the moulds. Throughout the filling process, in order to achieve the appropriate unit weight, the material was lightly vibrated and compacted with a rod in equal layers. After moulding the specimen at the targeted D_r , the upper and bottom end plates were clamped on tie rods.



Figure 2. Laboratory simulation of the grouting procedure.

The resin grouts with ER/W ratios of 1.5, 2.0 and 3.0 had constant viscosity values (Newtonian fluid) of 60, 75 and 85 cp, respectively, which were obtained using a capillary tube viscometer [25] at shear strain rates of up to 8000 s^{-1} . Despite the high viscosity values, all grouts easily penetrated the sand columns, even the columns of the finer sand, when pressure was exerted in the range of 1–2 bar. In order to achieve a more uniform grout flow and to prevent any fingering effects that could result from top-to-bottom flow, the grouts were injected from the bottom of the sand column. During the injection experiments, the volume of grout that was passing through the specimen was unceasingly measured using a digital flow meter. When excess grout, equivalent to 120% of the sand pore volume, had passed and collected from the outlet hose of the column, the grouting process was ceased. The grouted specimens were allowed to cure in the moulds in laboratory conditions for a period of at least 2 days, to develop adequate strength levels. Afterwards, they were demoulded and cut into smaller equal parts with a length of 11 cm. Thereafter, the samples were stored and cured in a moist room at a temperature of $20 \pm 3 \text{ }^\circ\text{C}$ and relative humidity of 95%, until the day of testing. These specimens were employed in UCS tests after 3, 7, 30, 90 and 180 days of curing in order to evaluate the increase in compressive strength and elastic modulus with time, as well as unconfined creep strength tests after 180 days of curing. Past research [18,20,23] has reported the detrimental influence of water withheld by the hydrophilic parts of the ER on the early strength development, since it inhibits the reaction between the ER and hardener. This negative impact diminishes over time because of the evaporation of water and the subsequent acceleration of the polymerisation process, resulting in a marginal strength improvement for curing periods greater than 90 days, since most of the quantity of ER and hardener has been polymerised earlier. However, it was decided to investigate the mechanical properties of treated sands at curing ages of up to 180 days. This decision was made because the grouts utilised in this study had higher ER/W

ratios than those of the grouts referred to in past studies, a fact that could influence the duration of the polymerisation reactions, resulting in the extension of the hardening process of polymer films beyond 90 days. All the UCS tests were carried out under a constant axial strain rate of 0.1%/min in accordance with the ASTM D 4219-02 [26] standards. The tests were carried out using a servohydraulic testing machine, incorporating a load cell (accuracy 10^{-5} N) and a linear variable displacement transducer (accuracy 10^{-5} mm), connected to a data logger/computer system for the recording of compressive stress–axial strain values during the test (Figure 3). The slope of the initial linear part of the stress–strain curve was used to compute the initial tangent modulus (elastic modulus).

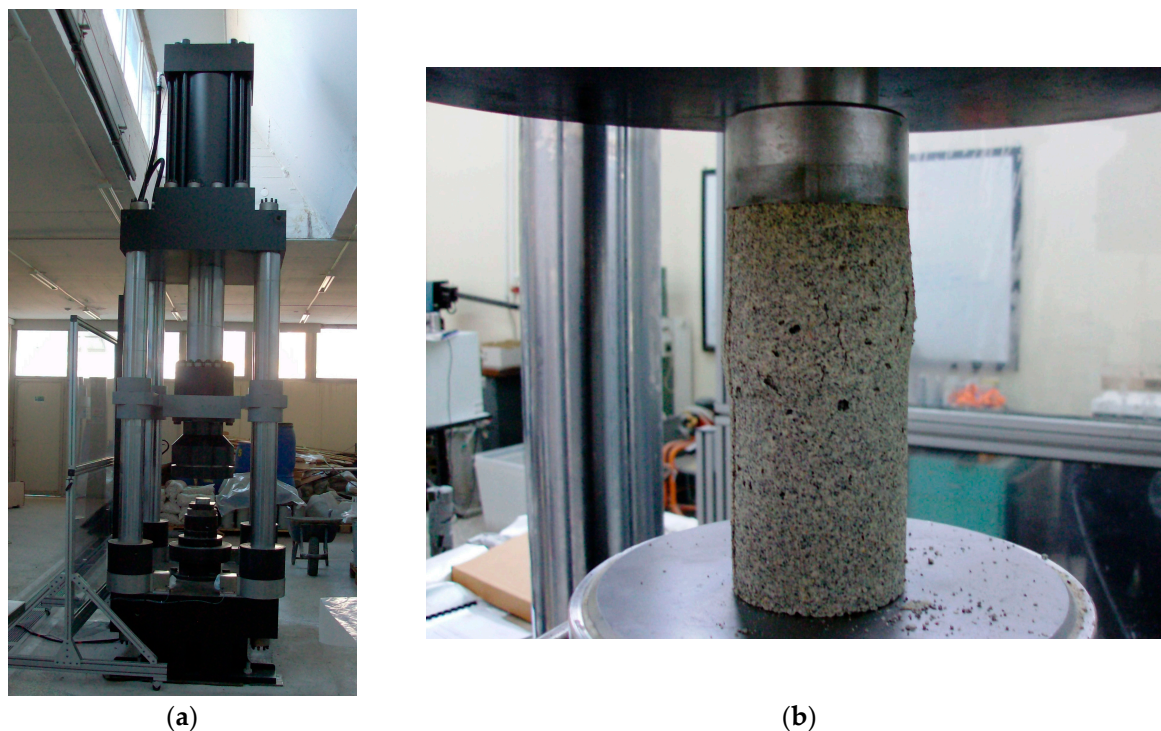


Figure 3. (a) Machine for compression strength tests; and (b) UCS test.

Long-term unconfined compression creep tests were performed on specimens of the same size and shape as the ones used for unconfined compression tests (also cured for 180 days). Creep tests were carried out in lever-type loading equipment (modified consolidation apparatus) that was capable of receiving a sample measuring 5.5 cm in diameter and 11.0 cm in height (Figure 4a). Each specimen was subjected to a constant loading expressed as a percentage of the compressive strength. After the start of the loading, the axial strain measurement was recorded at 1 min intervals for the first hour, then every hour for the first day and then every day until the end of the test. The maximum test time was three months. The axial deformation was measured with a 10^{-3} mm dial gauge. To study the effect of moisture on the deformation behaviour of grouted sands under permanent loading, two kinds of test were conducted: creep tests with different loading levels ranged from 50 to 90% of compressive strength on dry specimens and then on specimens immersed in water during the loading period (Figure 4b).

Porosity measurements of un-grouted sands were carried out according to the method proposed by Neithalath et al. [27]. In this method, the dry mass (M_1) of a sand sample contained in a plastic cylindrical tube (9.5 cm in diameter and 15.0 cm long) was weighed. Afterwards, water was added on the top of the sample until it was full. The mass of the saturated system (M_2) was then recorded. The difference between M_2 and M_1 gave the mass of the water in the pores. By converting this mass into a volume and expressing it as a percentage of the total volume of the sample, an indication of the total porosity was obtained.



(a)



(b)

Figure 4. Single lever consolidation apparatus for creep tests: (a) dry conditions; and (b) wet conditions.

The porosity of the grouted specimens was determined according to the saturation method suggested in ISRM with the use of a vacuum saturation device (Figure 5). Porosity was calculated using the following equation:

$$n = \frac{(M_{\text{sat}} - M_s) / \rho_w}{V} \times 100 \quad (1)$$

where M_s is the dry mass of the specimen, M_{sat} is the surface-dry saturated mass, V is the volume of the specimen and ρ_w is the density of water.



Figure 5. Vacuum saturation device for porosity measurements of grouted sands.

For the evaluation of water permeability of un-grouted sands, the constant head method was adopted, in accordance with ASTM D 5084-03 [28]. Figure 6 presents the set-up for the permeability tests. The coefficient of permeability k is given by:

$$k(\text{m/s}) = \frac{Q \cdot L}{A \cdot \Delta h} \quad (2)$$

where Q is the water flow (m^3/s), A is the cross section of a cylindrical specimen, Δh is the hydraulic height difference (m) and L is the sample height.



Figure 6. Set-up for determination of permeability coefficient of pure sands.

In the case of grouted sands, the constant head method was also performed for the determination of k . Specimens of the same size as the ones used for mechanical tests were placed in a triaxial cell. Triaxial permeability tests were carried out with a back-pressure system for ensuring the constant head approach and the direction of water flow, a flow meter and a confining pressure of 1 bar. k was calculated from the constant flow rate induced by the pressure difference across the specimen using Equation (2).

4. Results and Discussion

The results of the injection experiments demonstrated that all the ER grouts, when applied at relatively low pressure, could be easily propagated through the sand columns of the different grain sizes, even those made with the finer gradations. These observations are in agreement with the statements made in previous research [20,23], indicating that ER grouts have satisfactory penetrability characteristics, resulting in an isotropic strength development when injected into a soil mass. Some of the above findings are illustrated in Figure 7, which presents the results from compression tests that were performed on specimens extracted from different parts of the S_5 grouted sand columns, with grouts having an ER/W ratio of 3.0 and 1.5, and aged 90 days. In general, laboratory strength tests evidenced that compressive strength and elastic modulus values were almost equal and

unaffected by the distance between the inlet and outlet point of the grouted column for all of the grouted sands with the different grouts.

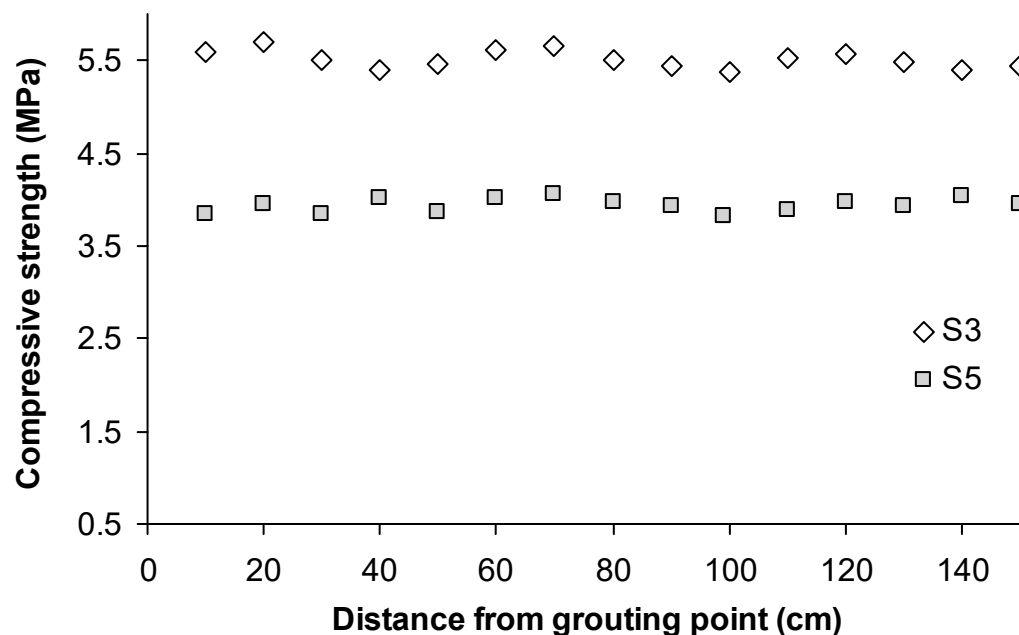
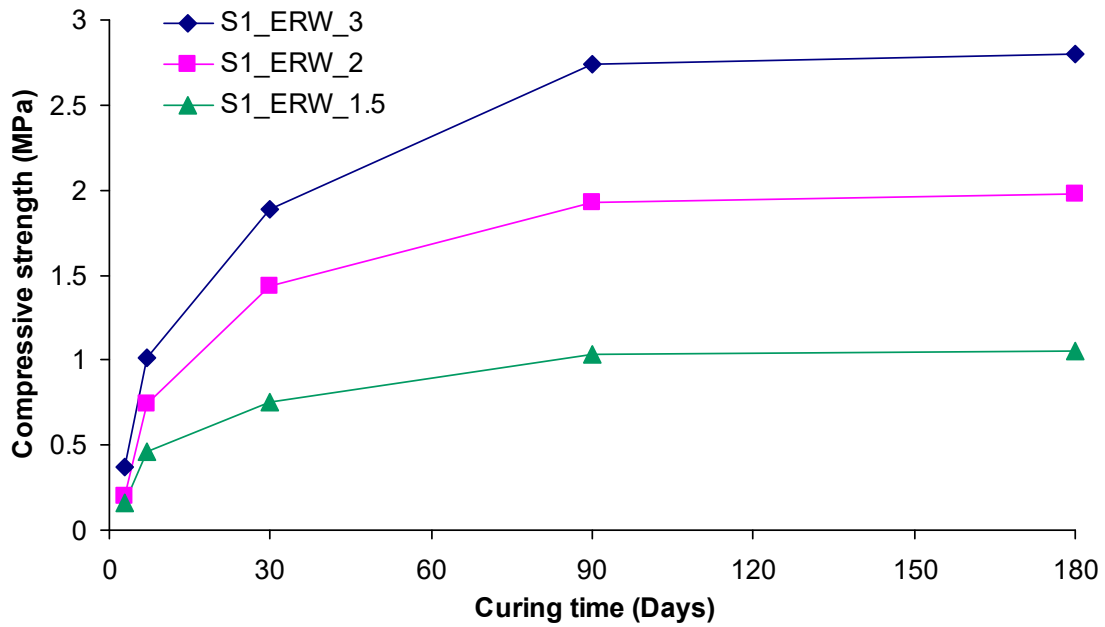


Figure 7. Compressive strength vs. distance from injection point for S₅ and S₃ sand treated with grout with ER/W ratio equal to 3.0.

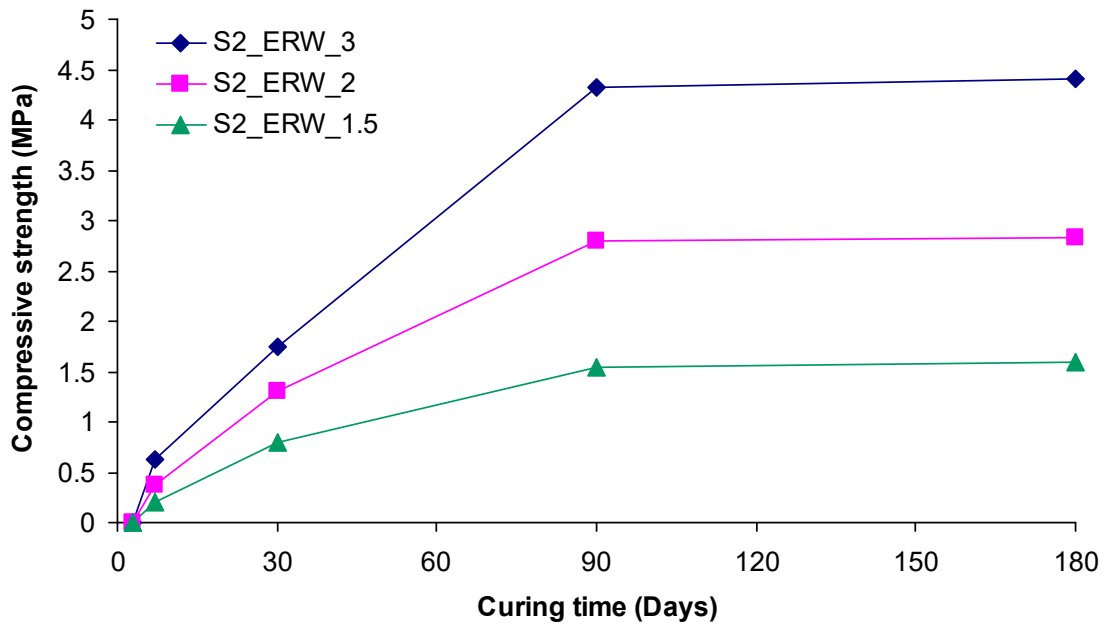
The compressive strength and elastic modulus values of grouted sands with various ER/W grouts, as a function of curing time, are depicted in Figures 8 and 9. It is clearly seen that strength values increased over time and the largest part of the strength was developed at the time interval between 7 and 90 days of curing. For higher curing periods, marginal increases in strength were obtained. A typical case, conforming to the above conclusion, is that of S₃ sand, with an ER/W grout ratio of 3.0; it appeared to have a 90-day compressive strength and elastic modulus which was 720 and 555% higher than those obtained at 7 days of curing, respectively. Irrespective of the distinct upward trend of strength over time, culminating in a marked elevation of its values, the detrimental effect of water in strength development at any curing age is obvious. This effect was heavily contingent upon the water content. In general, the lower the water content, the higher the strength of the grouted sands. For example, the 180-day compressive strength and elastic modulus of S₂ sand grouted with an ER/W ratio of 3.0 were 175 and 140% higher than those of S₂ when grouted with grout of an ER/W ratio equal to 1.5. The harmful effect of water on the strength development of grouted specimens may be due to the amount of water absorbed by the hydrophilic groups grafted on the molecular chain of ER, since it prohibits, to some extent, the reaction of resin with amine hardener [29]. Another explanation is the permanent weakness of the polymeric network, due to a partial hydrolysis of the ether linkages [15].

Figure 10 shows the stress–strain curves obtained from 180-day compression tests on specimens of S₃ sand grouted with grouts of an ER/W ratio equal to 3.0, 2.0 and 1.5. These curves are typical of the mechanical response exhibited by all grouted sands, with grouts of different ER/W ratios and at all curing ages. For all of the grouted sands considered in this research, the shape of the stress–strain curves demonstrated an initial elastic segment, followed by a large plastic zone extended in the pre- and post-failure region over a large range of strains. During the testing of all specimens, no sudden fracture was observed, even when shear bands (in fewer cases, related mainly with the lower ER/W ratio or the coarser sand) or excessive lateral bulging (in most cases) were visible. Specimens were continuously deformed until the test procedure was terminated, up to a strain of at least 3%. This ductile response reveals the domination of the strain-hardening behaviour of the ER

through a strong interfacial adhesion between the polymer membrane and sand grains on the deformation characteristics of the whole composite material, suggesting its application in earthworks or other geotechnical structures that may suffer significant deformations. Also, the results of this study indicate that ER grouts could offer suitable solutions for tunnelling technology, especially in the case of a tunnel construction in unstable fine soil deposits.

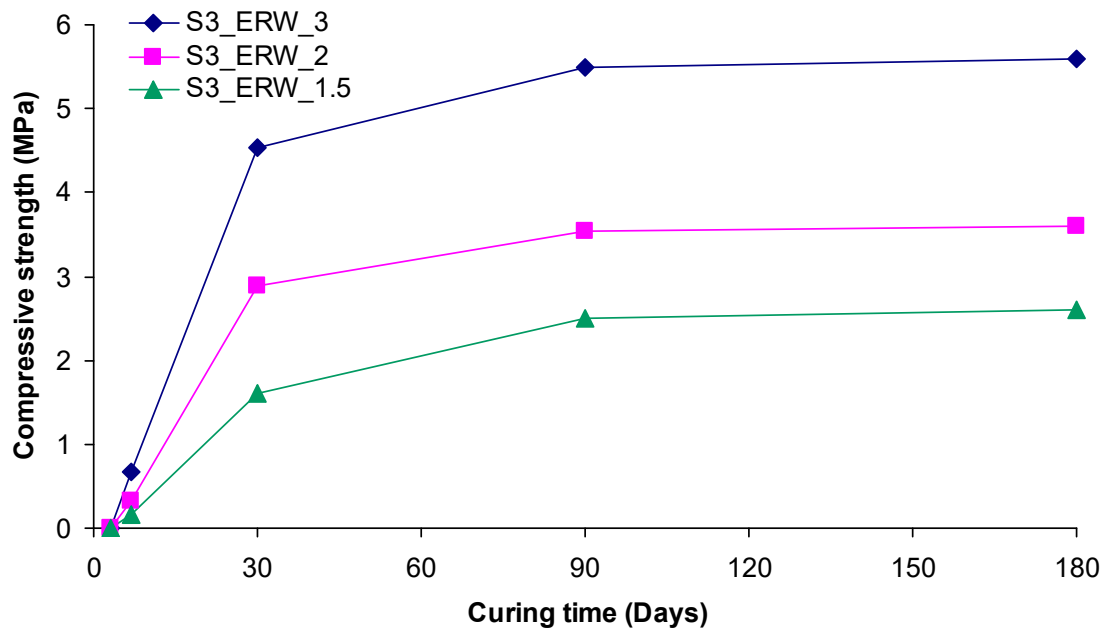


(a)

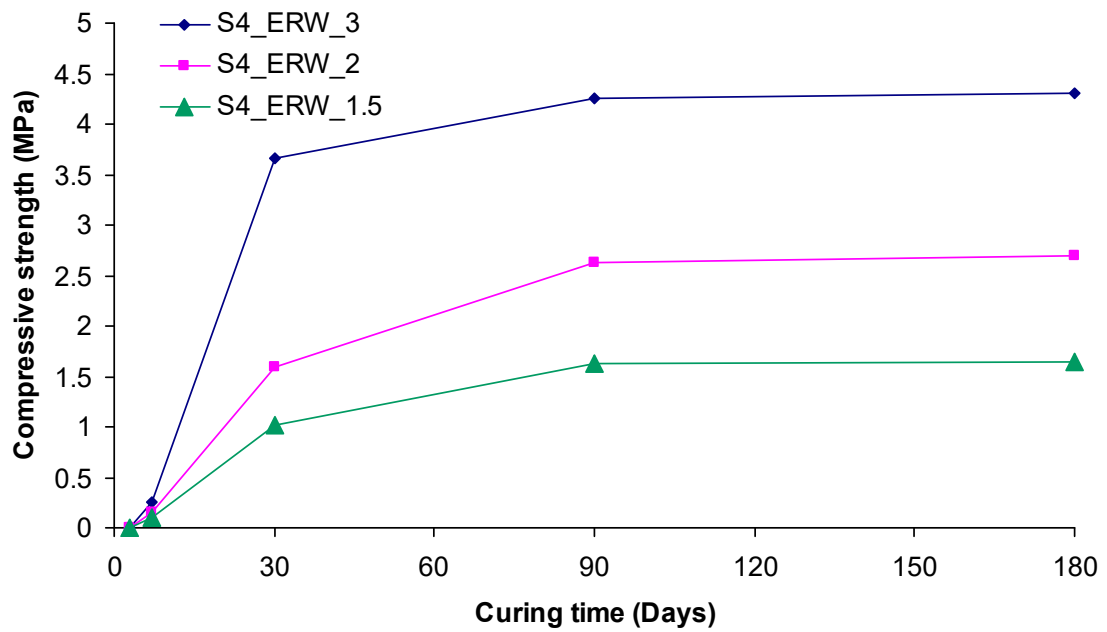


(b)

Figure 8. Cont.

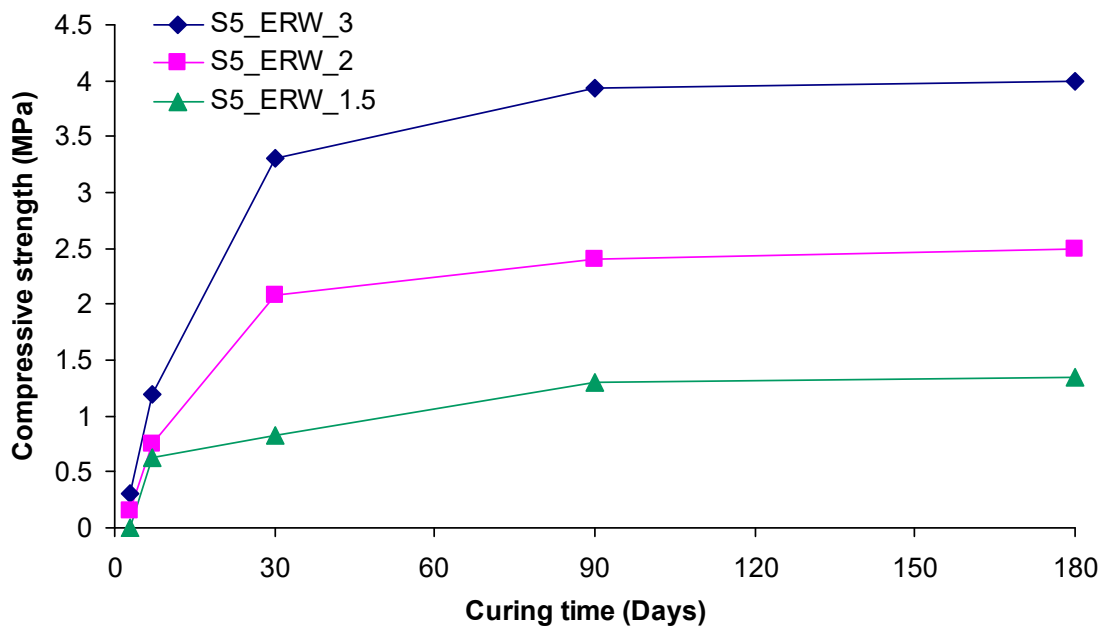


(c)

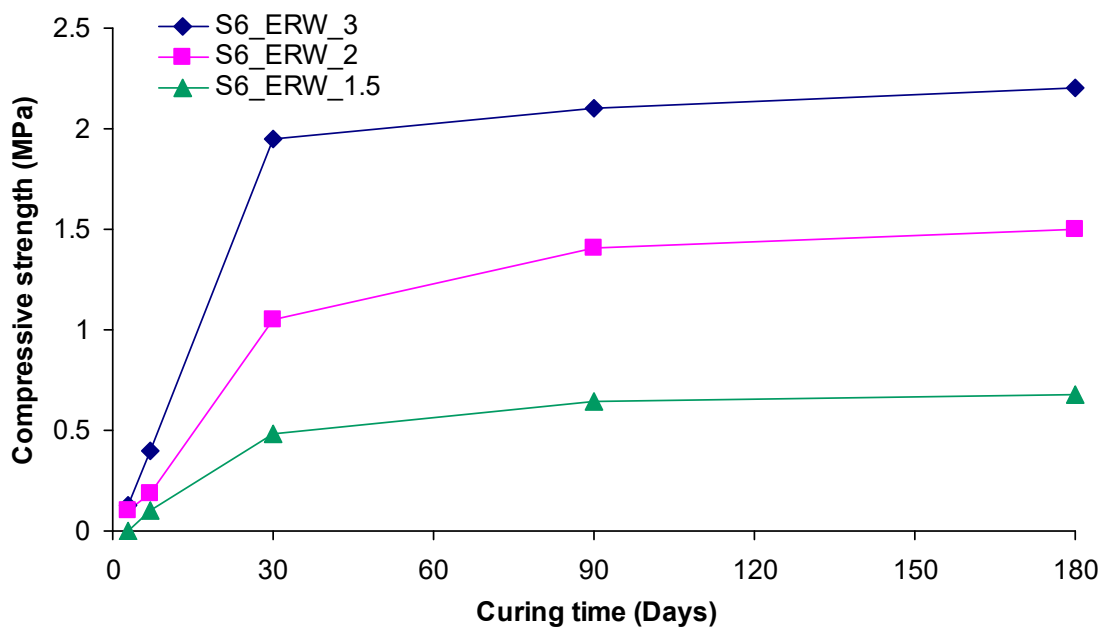


(d)

Figure 8. Cont.



(e)



(f)

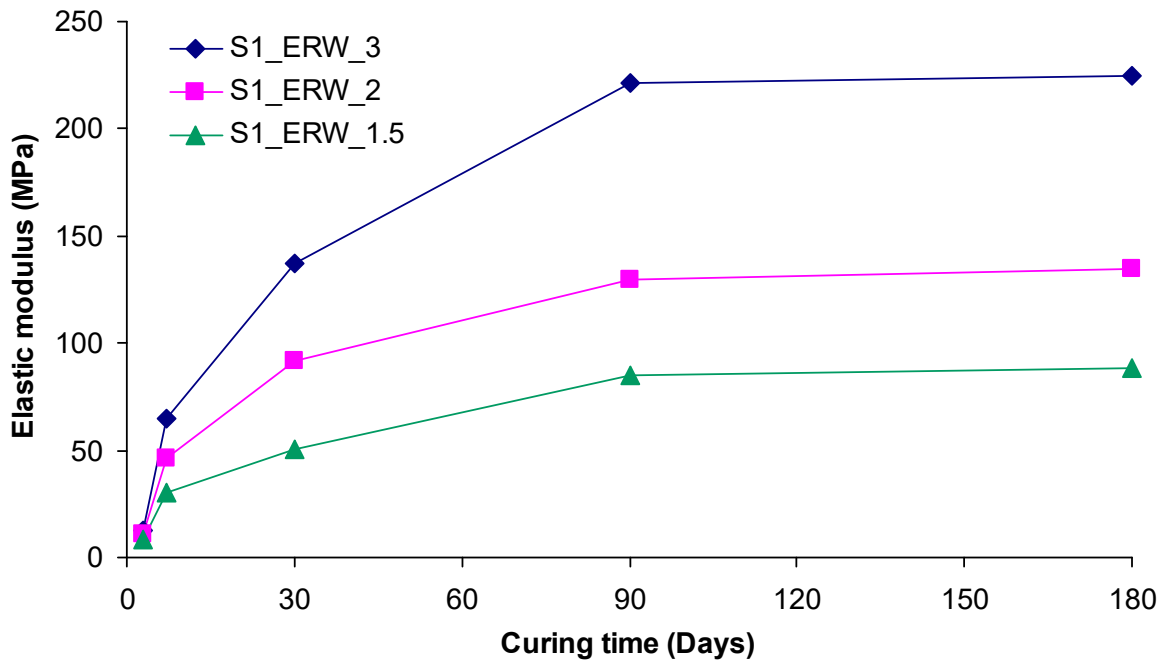
Figure 8. (a–f) Development of compressive strength with time for treated sands with the different grouts.

Figures 11 and 12 illustrate the relation between the strength parameters of grouted sands with the different resin grouts at a curing age of 180 days. It can be seen that there is a significant influence of d_{50} on the measured strength values. For example, the compressive strengths of S_3 sand (the finer sand) and S_6 sand (the coarser sand) grouted with grouts of ER/W ratios equal to 3.0 were 5.5 and 2.1 MPa, respectively. In the case of grouting with grouts having lower ER/W equal to 1.5, the effect of d_{50} on strength development is more pronounced; the compressive strength of S_3 sand appeared to be 3.9 times higher than that of S_6 sand. An explanation is that a decrease in the grain size of sands, or an increase in their specific surfaces, leads to an increase in the number of inter-particle contacts per unit volume and more surfaces for bonding are provided for the grouts. In general, for all ER/W

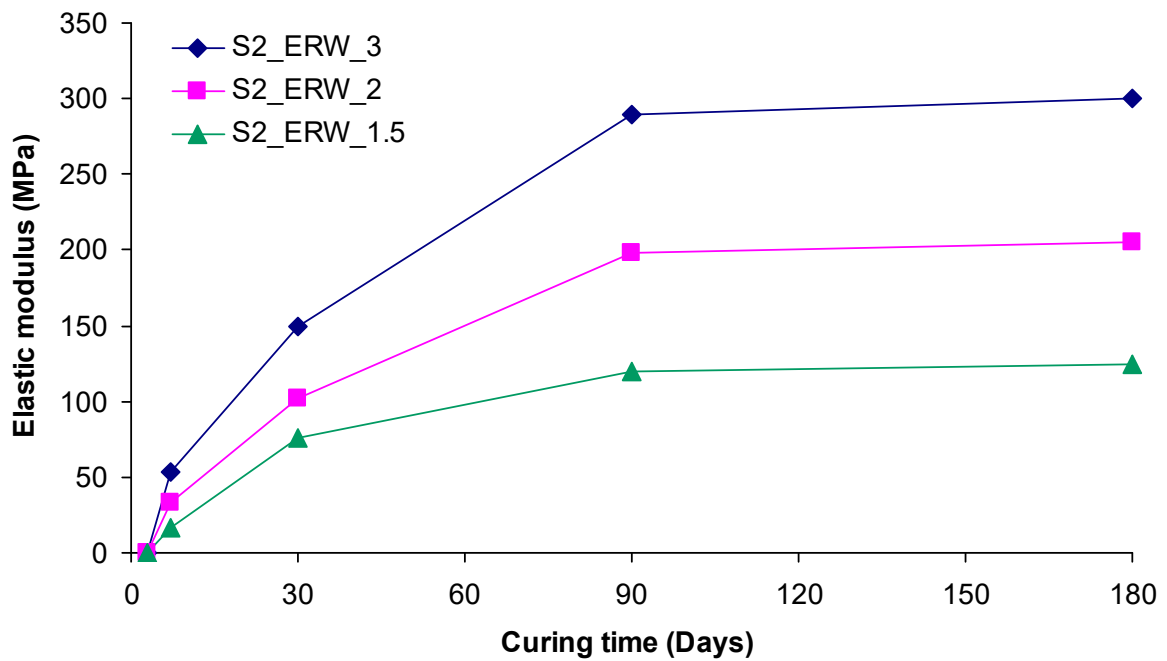
ratios, a reduction in the d_{50} of the sands results in a considerable enhancement in strength properties of the grouted sands. For the S_3 , S_2 , S_1 and S_6 sands, having a similar coefficient of uniformity (c_u) value, the proportion among the two factors is accurately described by the power law as:

$$\text{UCS or EM} = a d_{50}^b \tag{3}$$

where UCS is the unconfined compressive strength (MPa) at 180 days of curing; EM is the elastic modulus (MPa) at 180 days of curing; d_{50} is the mean grain size of sand (mm) and a and b are coefficients determined from regression analysis. Table 2 summarises the values of the fitting parameters and R^2 for all ER/W ratios.

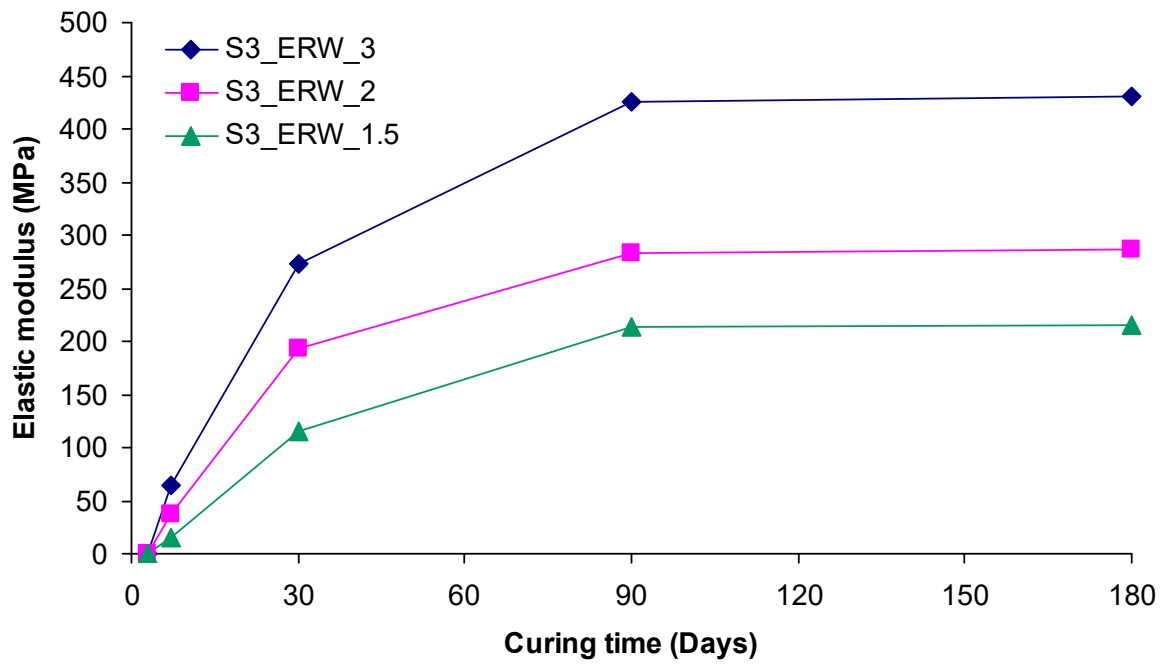


(a)

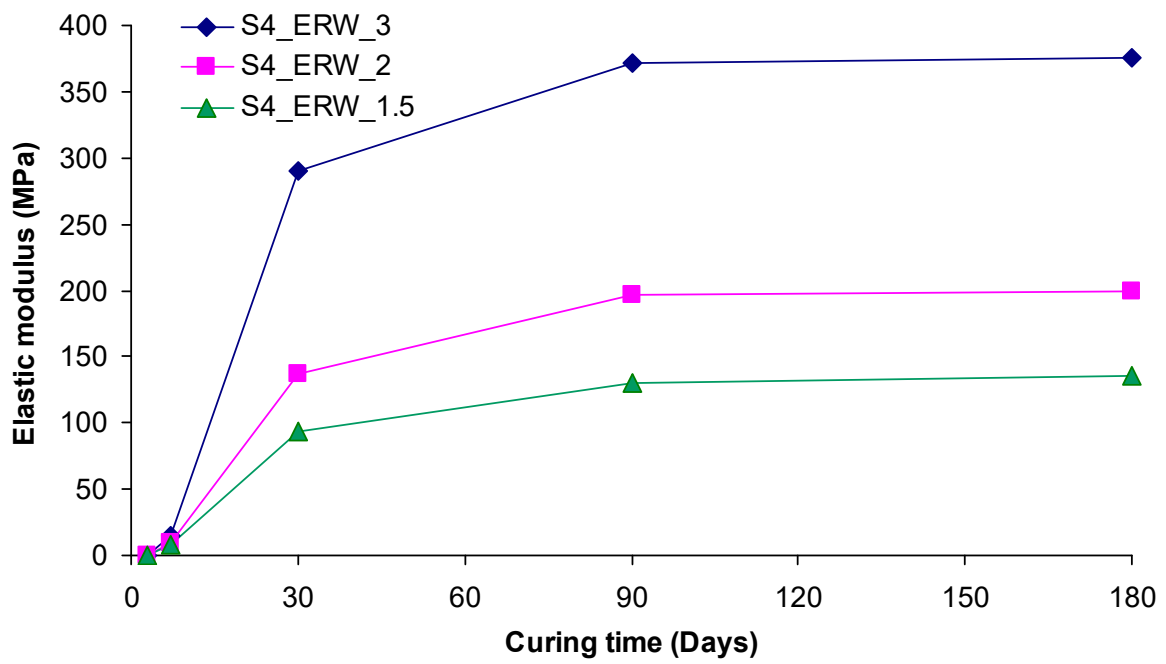


(b)

Figure 9. Cont.

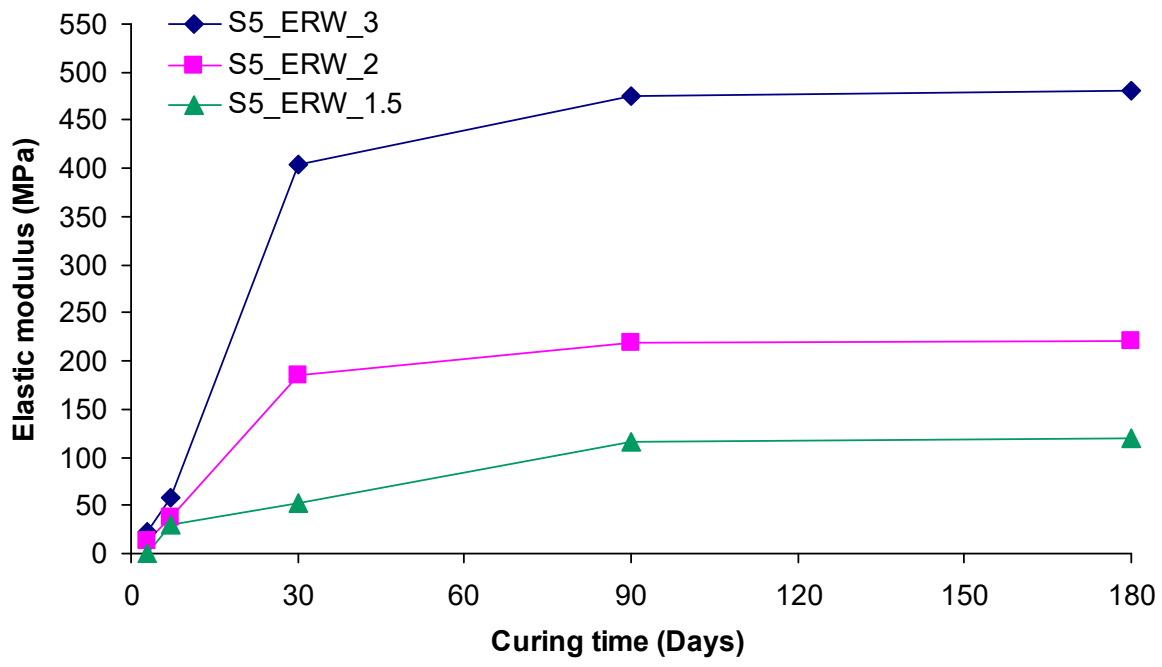


(c)

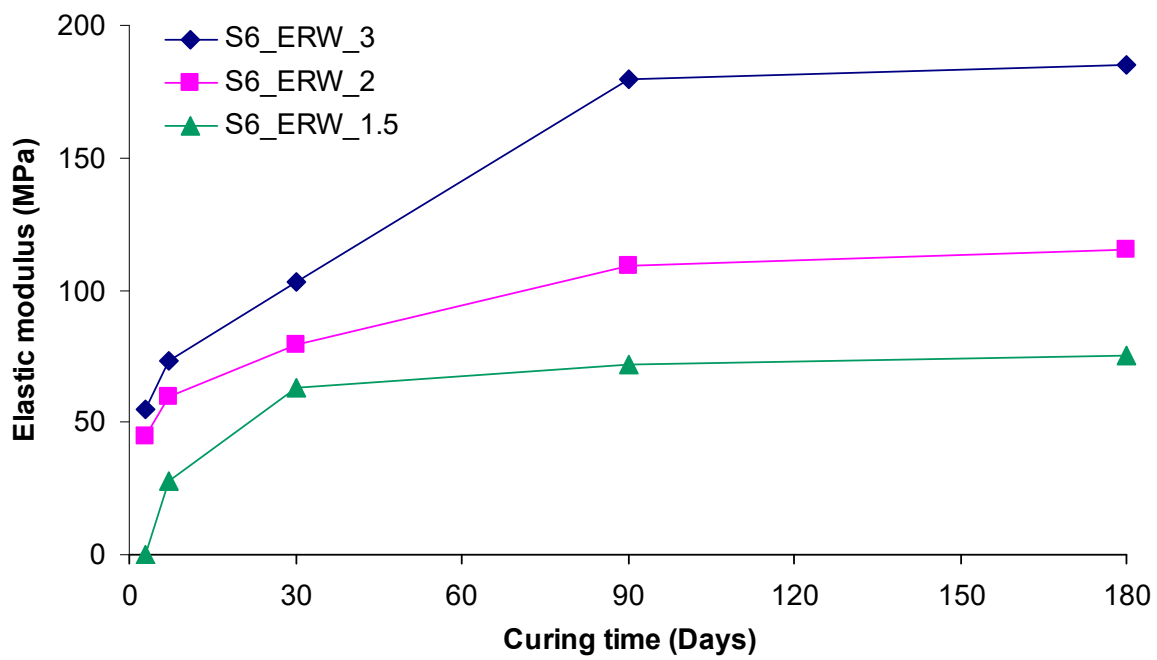


(d)

Figure 9. Cont.



(e)



(f)

Figure 9. (a–f) Development of elastic modulus with time for treated sands with the different grouts.

Table 2. Values of regression coefficients and R².

ER/W Ratio	a		b		R ²	
	UCS	EM	UCS	EM	UCS	EM
3	2.543	206.66	−0.324	−0.272	0.99	0.95
2	1.726	126.05	−0.304	−0.313	0.99	0.96
1.5	0.852	82.08	−0.432	−0.339	0.98	0.92

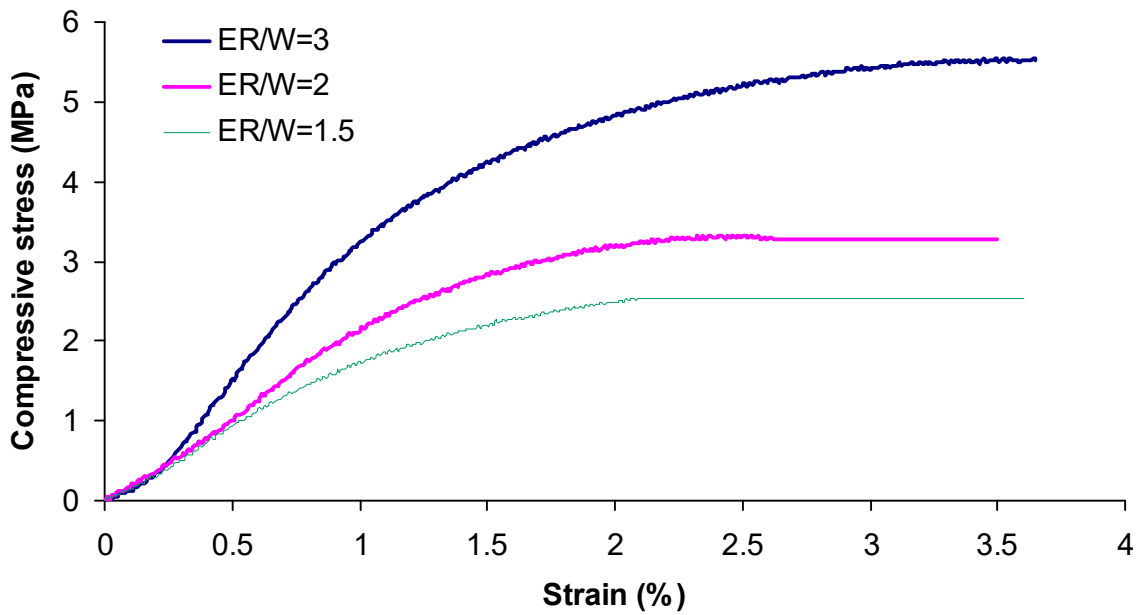


Figure 10. Typical curves of compressive stress vs. strain for S₃ sand samples treated with the different grouts after 180 days of curing.

The curves in Figures 11 and 12 show a consistent relation between mechanical indices and d_{50} . However, in the case of S₄ and S₅ sands, with c_u values much higher than those for other sands, their data in the graphs shifted upward with respect to the curves. This reveals the significant influence of c_u on the strength of the grouted sands. Obviously, the change in strength is directly related to the distribution of grains of different sizes in the soil mass, interlocking with each other to form a more unitary matrix and an increased number of contacts, providing more surfaces for the grouts to develop bond interfacial strength.

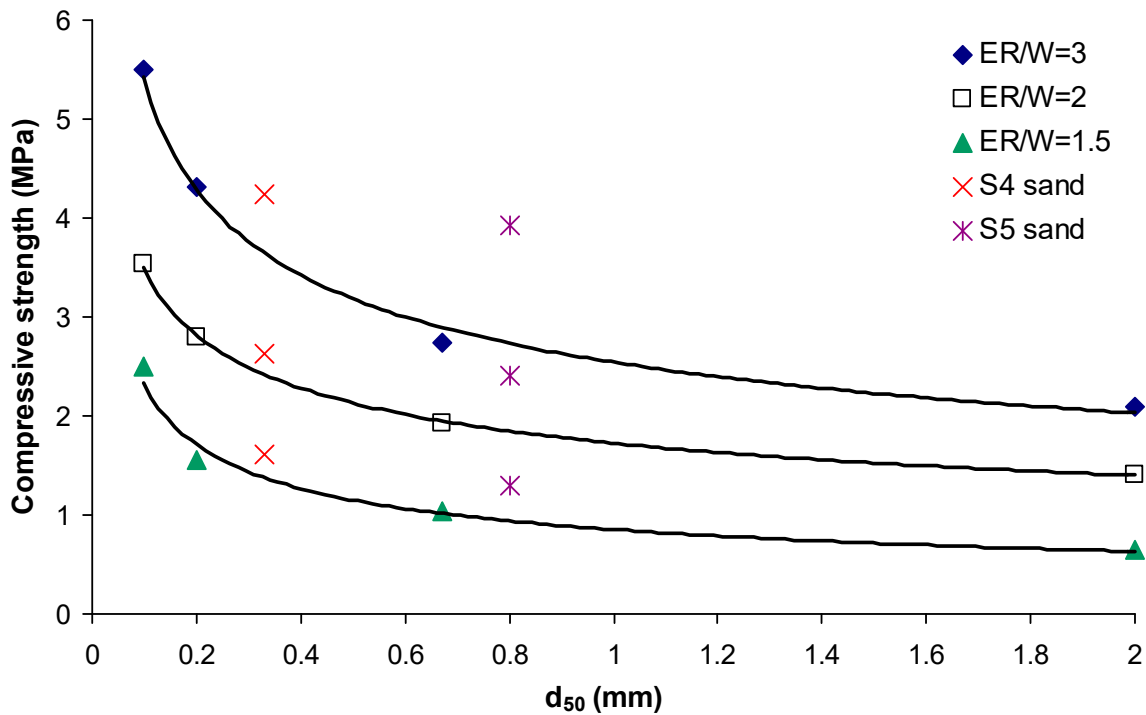


Figure 11. Compressive strength vs. mean grain size of all grouted sands after 180 days of curing.

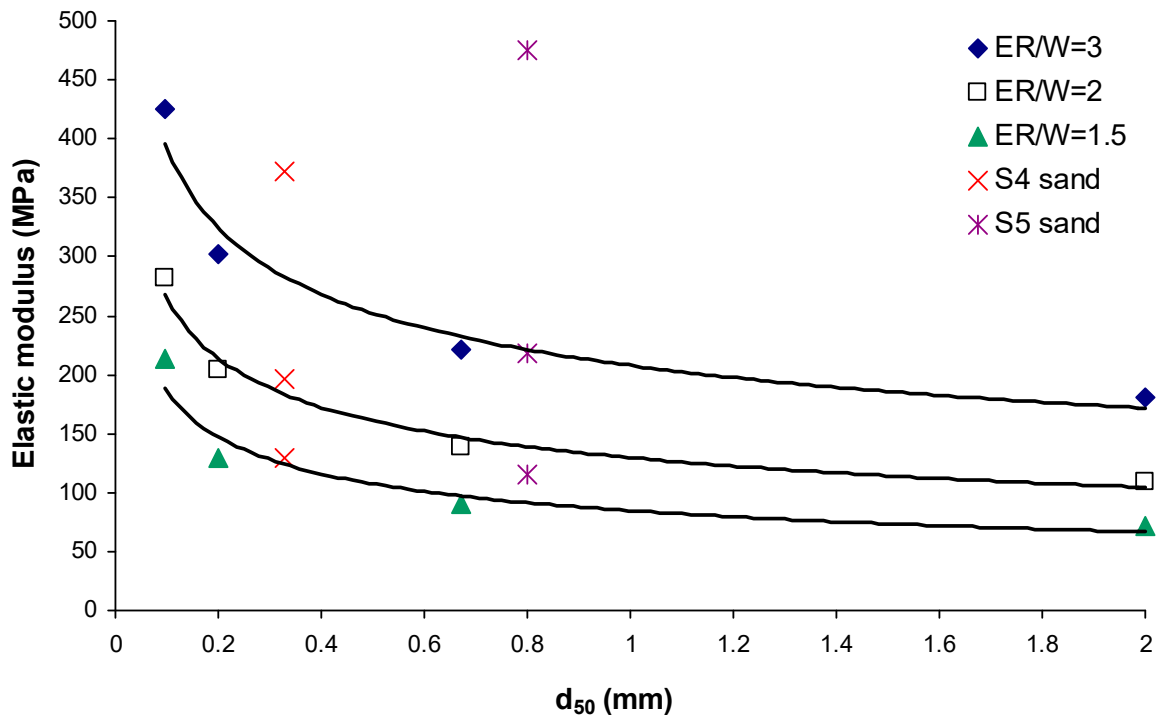


Figure 12. Elastic modulus vs. mean grain size of all grouted sands after 180 days of curing.

Table 3 summarises the experimental values of the porosity for all the untreated and treated sands. For each of the six sands, the higher the ER/W ratio, the lower the porosity of the grouted sand. However, a general trend relating the strength and porosity of all the grouted sands was not detected. In Figure 13, the values of the compressive strength are plotted against the values of porosity. This comparison of porosity and strength test measurements for the different grouted sands reflects the lack of any relation between the two factors. For instance, the porosity of the finer sand S_3 (from which the higher strength values were obtained) and the coarser sand S_6 (from which the lower strength values were obtained) was 37.04 and 34.50%, respectively, when injected with grouts having an ER/W ratio of 3.0. These experimental results provide more evidence that the reinforcement efficacy of ER grouts is strongly dependent on the number of grain-to-grain contact points, a fact that is related to d_{50} and c_u , as referred to previously. From an economic point of view, it should be mentioned that, although epoxy resin is slightly more expensive than other conventional grouting materials, the small amount of resin required for improving the soil to be grouted implies that its share of the total cost for the ground improvement operation is very low. Hence, it is worth utilising. Indeed, the current results show that the reduction of porosity for all grouted sands was low and ranged from 6.9 to 29.0%.

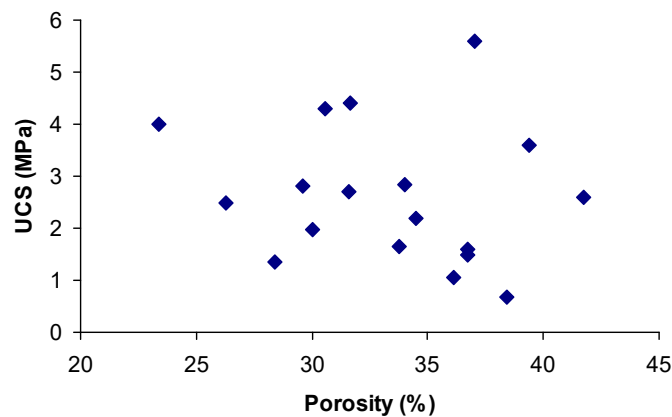


Figure 13. Porosity vs. UCS of grouted sands.

Table 3. Coefficient of permeability and porosity values of un-grouted and grouted sands.

Notation	k (m/s)	n (%)
S ₁	3.04×10^{-3}	41.7
S ₁ + ER/W = 3	4.72×10^{-6}	29.62
S ₁ + ER/W = 2	8.29×10^{-6}	30
S ₁ + ER/W = 1.5	1.03×10^{-5}	36.14
S ₂	2.89×10^{-4}	43.4
S ₂ + ER/W = 3	2.6×10^{-6}	31.68
S ₂ + ER/W = 2	6.1×10^{-6}	34
S ₂ + ER/W = 1.5	7.34×10^{-6}	36.7
S ₃	4.94×10^{-5}	45.4
S ₃ + ER/W = 3	8.76×10^{-7}	37.04
S ₃ + ER/W = 2	2.97×10^{-6}	39.41
S ₃ + ER/W = 1.5	8.72×10^{-6}	41.72
S ₄	7.04×10^{-5}	36.3
S ₄ + ER/W = 3	2.46×10^{-6}	30.56
S ₄ + ER/W = 2	3.5×10^{-6}	31.6
S ₄ + ER/W = 1.5	5.27×10^{-6}	33.79
S ₅	3.4×10^{-4}	32.6
S ₅ + ER/W = 3	9.68×10^{-7}	23.4
S ₅ + ER/W = 2	3.47×10^{-6}	26.3
S ₅ + ER/W = 1.5	9×10^{-6}	28.4
S ₆	9.56×10^{-2}	43.1
S ₆ + ER/W = 3	9.2×10^{-6}	34.5
S ₆ + ER/W = 2	1.2×10^{-5}	36.7
S ₆ + ER/W = 1.5	2.94×10^{-5}	38.4

Based on the experimental data, a non-linear regression analysis was conducted using a statistics software program. The analysis related the final strength indices of the grouted sands, UCS and EM (both in MPa), to the descriptor variables, including d₅₀ (mm), ER/W ratio and c_u. The performance of the regression yielded the following equations:

$$UCS = (d_{50}^{-0.34}) [-1 + (ER/W)^{0.001}] (3.74 + c_u^{3.53}), \quad R^2 = 0.98 \quad (4)$$

$$EM = 0.022 (d_{50}^{-0.33}) [-0.411 + (ER/W)^{1.178}] (2.83 + c_u^{3.84}), \quad R^2 = 0.95 \quad (5)$$

The relationships between the measured and predicted strength values from the regression formulas are visualised in Figures 14 and 15.

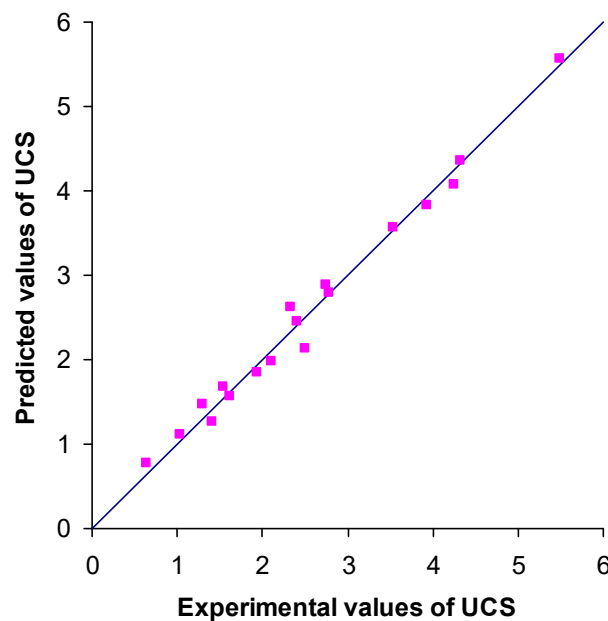


Figure 14. Cross-plot of compressive strength values predicted from regression Equation (4) vs. one from laboratory tests.

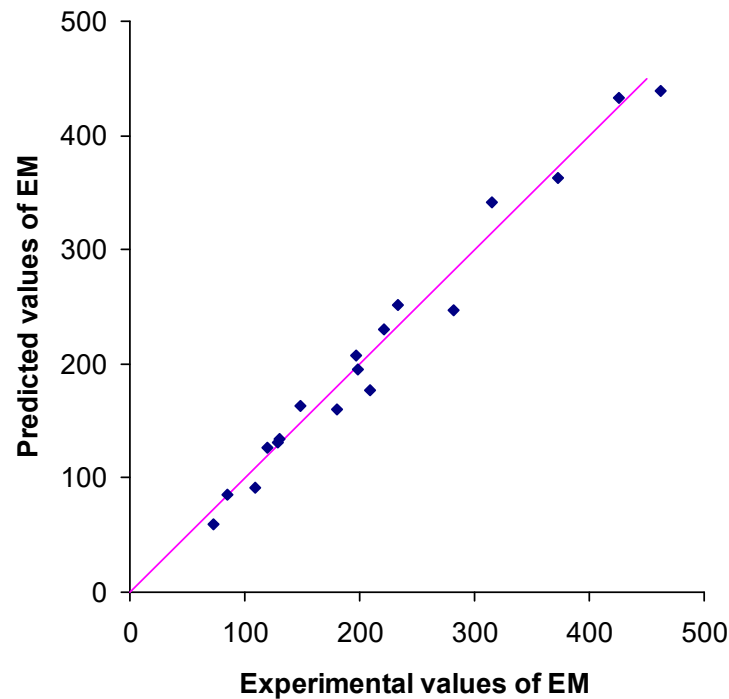


Figure 15. Cross-plot of elastic modulus values predicted from regression Equation (5) vs. one from laboratory tests.

The strength of grouted sands is affected by numerous factors, such as the proportions of water and cement, types of grout and curing time, the specific surface of both sand and cement, and the fines content, particle size, relative density and mineralogy of the sand [30–32]. The influence of mineralogical composition on the strength of grouted soils has been the subject of several studies, as shown by the research activity published in international scientific journals [33–35]. However, little research has been undertaken to examine its effect on the mechanical properties of ER-treated soils. Hamidi et al. [36] performed UCS tests on soils containing various clay mineral types. These tests showed that the efficiency of stabilisation with ER is strongly dependent on the type and percentage of clay minerals. Consequently, injection tests were also carried out on siliceous sand columns with grouts having ER/W ratios of 3.0, 2.0 and 1.5. The strength test results obtained for grouted siliceous sand at 180 days of curing are compared with those of S_1 calcareous sand (which has similar gradation and index properties to the siliceous sand) in Table 4. The comparison reveals an insignificant difference between the compressive strength and elastic modulus values of the two sands for all grouts proportioned using different ER/W ratios. However, since one type of sand has been utilised in this research effort, it is not possible to extend the current experimental results into a general conclusion and so more work needs to be undertaken on a wide range of soils.

Table 4. Strength parameters of the two sands.

ER/W Ratio	Compressive Strength (MPa)		Elastic Modulus (MPa)	
	Calcareous	Siliceous	Calcareous	Siliceous
3	2.8	2.66	225	230
2	1.98	1.88	135	128
1.5	1.05	1.1	88	92

Several authors have shown that the existence of a creep limit can be expressed as a stress level [37–40]. Soils remain stable when subjected to loadings lower than the creep limit; whereas, beyond this limit, soil exhibits large deformations and collapses over a short

or long time period. The creep limit Q_f assessment is based on the determination of the slope of the strain evolution over time, for each loading. The slope variation with loading consists of two or three linear parts. The creep limit is considered to be the stress value at which the transition between the two last parts occurs [38]. The above methodology for the estimation of Q_f was adopted in this current study, as depicted in Figure 16. For instance, the measurements of creep tests for S_1 sand grouted with grout of an ER/W ratio equal to 3.0 are illustrated in Figure 17, which presents the variation in creep strain over time for loading levels ranging from 70 to 90% of compressive strength (q_c), under dry conditions. Figure 18 represents the estimation of the Q_f from the a - q_c curve. The curve was plotted using the data for loading equal to 70, 75, 80 and 85% of q_c . For the estimation of Q_f , the loadings equal to 87.5 and 90.0% of q_c were omitted because rupture of the specimens at early stages was observed. Table 5 summarises the creep limit under dry and wet conditions for all grouted sands with the grouts of different proportions. Table 5 evidences that Q_f , determined under dry or wet conditions, increased slightly with the increase in ER/W ratio for each of the six sands. However, a general trend for all grouted sands is not identified, since their Q_f values are very close and independent of the d_{50} and c_u . An exception to this is the case of the coarser sand S_6 , the Q_f values of which are much lower when compared with the ones for the other sands. The comparison of these experimental results confirms the detrimental influence of water on the creep behaviour of all grouted sands. However, this negative impact of water resulted in a relatively small reduction in Q_f values, which ranged from 5.0 to 7.5% in total terms. For S_6 sand, this decrement in Q_f was more significant and fluctuated from 10 to 12%. The test results also indicate that the ER-grouted sands exhibited superior creep strength compared with other chemical grouts. For example, Ribay et al. [38] stated that sands grouted with silica gels have a Q_f of about 10%. Ata and Vipulanandan [37] showed that the Q_f of silicate grouted sand is below 50%. It should be mentioned that, currently, there is no published data about the creep behaviour of grouted sands with water-soluble epoxy resin solutions.

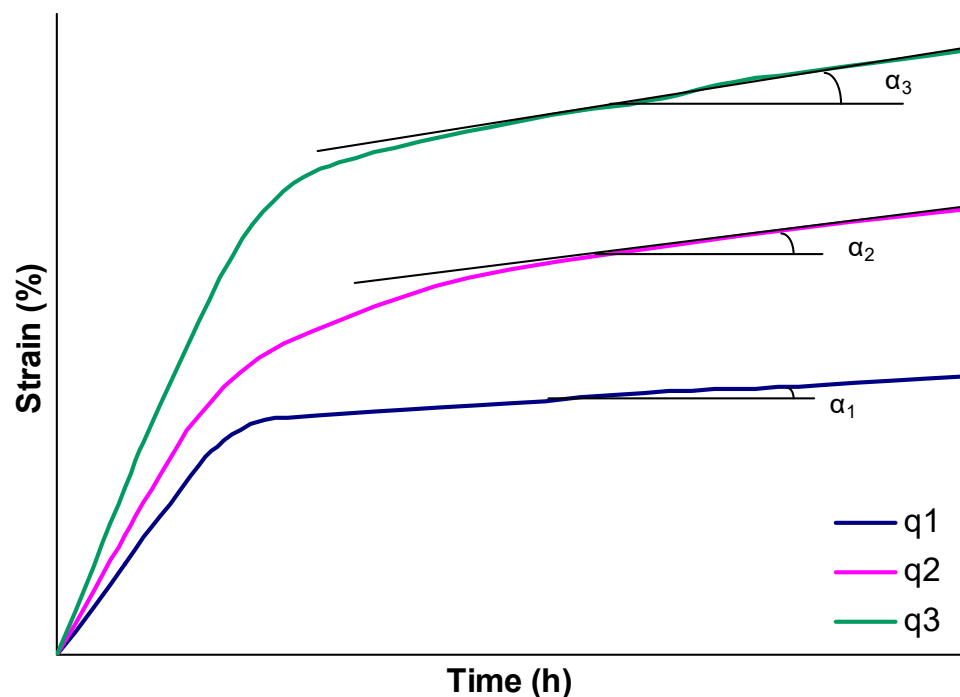


Figure 16. Cont.

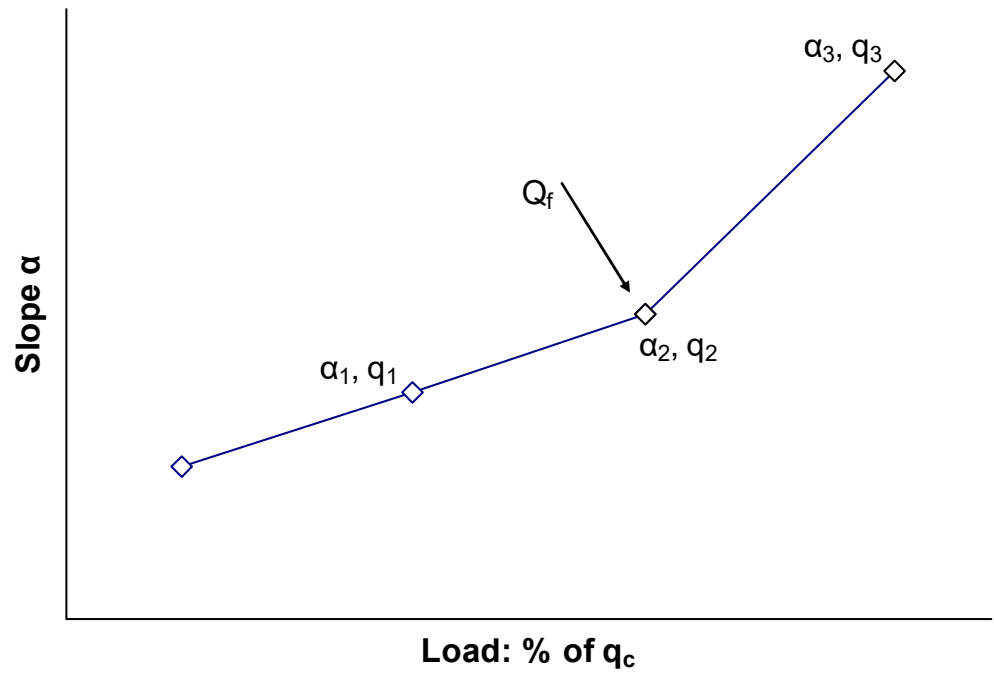


Figure 16. Method for the estimation of creep limit.

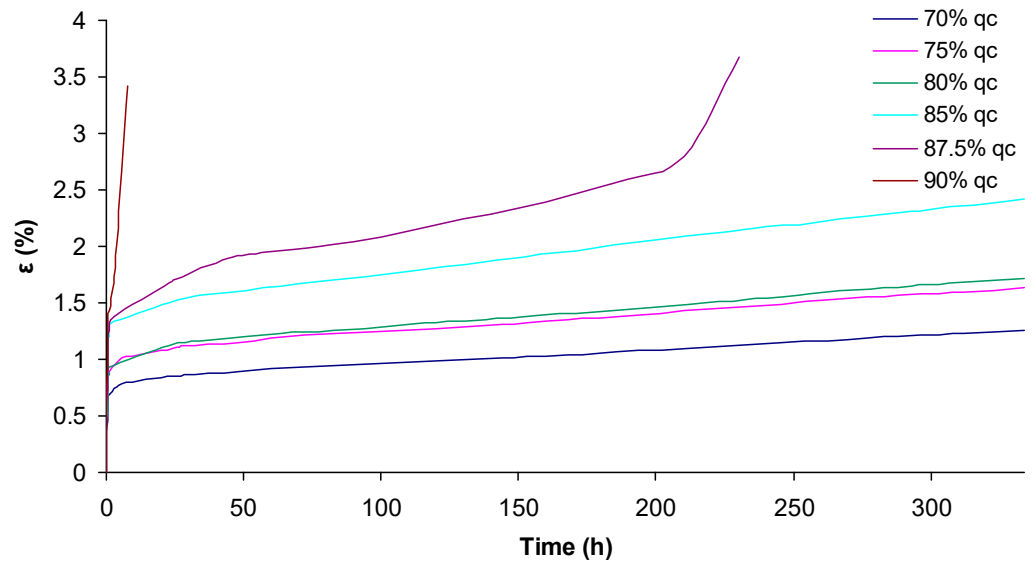


Figure 17. Unconfined creep tests for S₁ sand grouted with grouts of ER/W ratio equal to 3.

The values of k for un-grouted and grouted sands obtained from permeability tests are also included in Table 3. As for the mechanical properties, the reduction in water permeability was directly related to the ER/W ratio, d_{50} and c_u . In the case of grouting with the thicker grouts, permeability test results verify the accretion of a dense polymer membrane on the particle surface, which fills or seals a large number of pores, resulting in the significant reduction of k values. The most appreciable decrease in k was obtained for S₆ sand grouted with grouts of an ER/W ratio equal to 3.0, by four orders of magnitude; whereas the decrease in the values of k for the other grouted sands ranged from one to three orders of magnitude. In general, the values of k for all grouted sands are comparable with those obtained with other common chemical grouts [41].

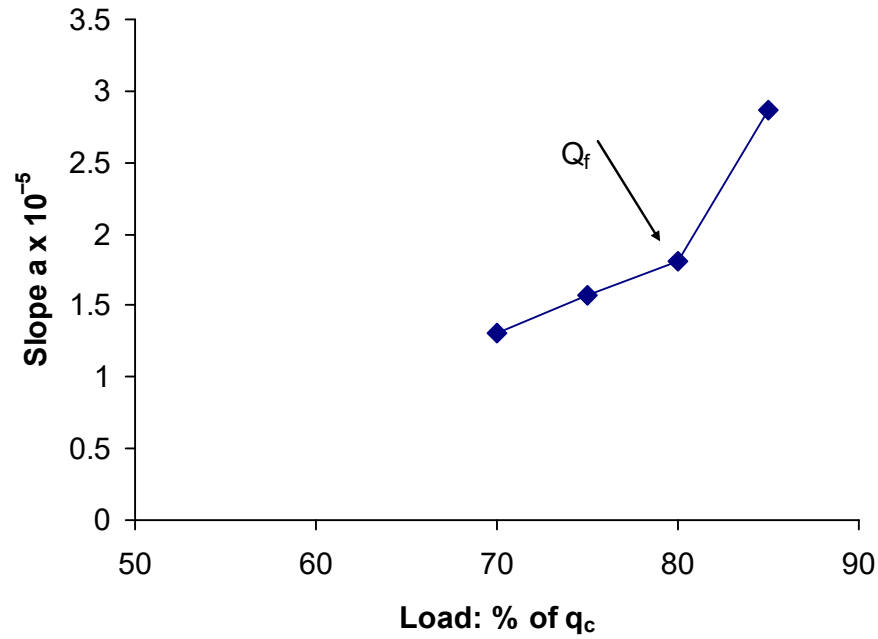


Figure 18. Creep limit for S_1 sand grouted with grouts of ER/W ratio equal to 3 under dry and wet conditions.

Table 5. Creep limit of grouted sands.

Notation	Q_f	
	Dry Condition	Wet Condition
$S_1 + ER/W = 3$	80	72.5
$S_1 + ER/W = 2$	77.5	70
$S_1 + ER/W = 1.5$	75	70
$S_2 + ER/W = 3$	82	75
$S_2 + ER/W = 2$	80	75
$S_2 + ER/W = 1.5$	78	72.5
$S_3 + ER/W = 3$	85	77.5
$S_3 + ER/W = 2$	82.5	75
$S_3 + ER/W = 1.5$	80	75
$S_4 + ER/W = 3$	82	75
$S_4 + ER/W = 2$	80	72.5
$S_4 + ER/W = 1.5$	80	72.5
$S_5 + ER/W = 3$	80	75
$S_5 + ER/W = 2$	78.5	72.5
$S_5 + ER/W = 1.5$	77.5	70
$S_6 + ER/W = 3$	72.5	62.5
$S_6 + ER/W = 2$	70	60
$S_6 + ER/W = 1.5$	67.5	55.5

On the basis of the experimental results, a regression analysis was carried out to correlate the k (m/s) of grouted sands to the descriptor variables, including ER/W ratio, d_{50} and c_u . The model that gives the best correlation is:

$$k = 3.26 \times 10^{-4} (d_{50}^{0.503}) [0.06 + (ER/W)^{-4.59}] (0.135 + c_u^{-4.48}), \quad R^2 = 0.96 \quad (6)$$

The relationship between the measured and predicted k values from the regression equation is illustrated in Figure 19.

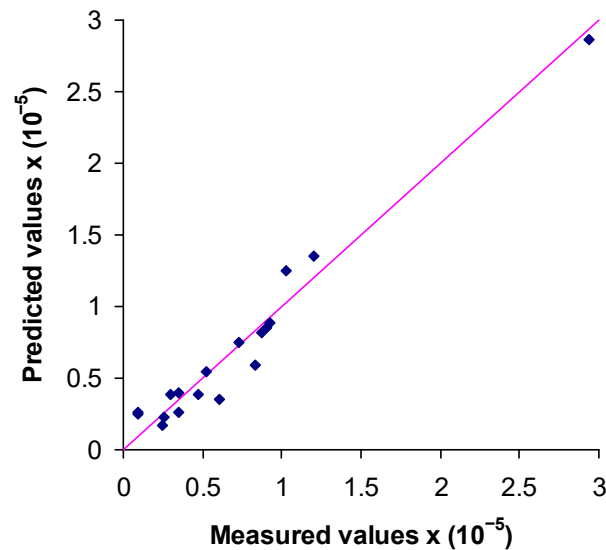


Figure 19. Cross-plot of k values predicted from the regression Equation (6) vs. one from laboratory tests.

5. Conclusions

Thorough experimental research was conducted to assess improvements to some physical and mechanical properties of a wide range of grouted sands with three different ER grouts. The effect of several factors on the outcome was investigated and important findings for designing injection projects utilising such material were obtained. The conclusions can be summarised as follows:

- (1) All grouted sands with the different grouts gain their final strength after 90 days of curing. The higher the ER/W ratio, the greater the strength development, at all curing ages.
- (2) The final compressive strength and elastic modulus of grouted sands depend directly on the ER/W ratio, d_{50} and c_u . The higher the ER/W ratio and c_u , and the finer the sand, the greater the strength development at all curing ages. In particular, the highest compressive strength and elastic modulus values at the age of 180 days are obtained for the finer sand (S_3), grouted with the different grouts, ranging from 2.6 to 5.6 MPa and 216 to 430 MPa, respectively. These values are much higher than those obtained by the use of other chemical grouts. On the contrary, the lowest compressive strength and elastic modulus values are obtained for the coarser sand (S_6) with a low c_u value, ranging from 0.68 to 2.2 MPa and 75 to 185 MPa, respectively, which are slightly higher but comparable to those achieved with common chemical grouts.
- (3) All the grouted sands considered in this study exhibit strain-hardening behaviour. This response suggests their potential application in geotechnical structures that may suffer significant deformations.
- (4) The mineralogical composition of sand does not seem to influence the strength development.
- (5) All the grouted sands have stable long-term creep behaviour with high values of Q_f ranging from 67.5 to 80% of q_c . These values are higher than those obtained with other chemical grouts. Even under the adverse influence of water, the reduction of the Q_f values is very low in most cases.
- (6) The permeability of the grouted sands decreases by two to four orders of magnitude when the grouts are injected into fine sands or sands with high c_u . However, the values of k for all the grouted sands are comparable to those obtained with other chemical grouts.
- (7) The models derived from non-linear regression analysis relate the UCS, EM and k of the grouted sands to the ER/W ratio, d_{50} and c_u . The predictive accuracy of the regression equations was found to be remarkably high.

It may be concluded that the use of ER grouts in fine sands or well graded sands can be much more effective than the utilisation of the other so far known chemical grouts and could give suitable solutions in many geotechnical works such as foundations, tunnels, dams, soil nailing, stabilisation of deep excavations, etc.

Author Contributions: Both the co-authors contribute equally for designing the experiments, analysing the data, writing the manuscript, revisions and editing. All authors have read and agreed to the published version of the manuscript.

Funding: This research received no external funding.

Data Availability Statement: The data are contained within this article.

Conflicts of Interest: The authors declare no conflicts of interest.

References

1. Celik, F. The observation of permeation grouting method as soil improvement technique with different grout flow models. *Geomech. Eng.* **2019**, *17*, 367–374.
2. Saleh, S.; Yunus, N.Z.M.; Ahmad, K.; Ali, N. Improving the strength of weak soil using polyurethane grouts: A review. *Constr. Build. Mater.* **2019**, *202*, 738–752. [[CrossRef](#)]
3. Anagnostopoulos, C.A. Laboratory study of an injected granular soil with polymer grouts. *Tunn. Undergr. Space Technol.* **2005**, *20*, 525–533. [[CrossRef](#)]
4. Anagnostopoulos, C.A. Physical and mechanical properties of injected sand with latex-superplasticized grouts. *Geotech. Test J.* **2006**, *29*, 490–496.
5. Gallagher, P.M.; Lin, Y. Colloidal silica transport through liquefiable porous media. *J. Geotech. Geoenvironmental Eng.* **2009**, *135*, 1702–1712. [[CrossRef](#)]
6. Ajalloeian, R.; Matinmanesh, H.; Abtani, S.M.; Rowshanzamir, M. Effect of polyvinyl acetate grout injection on geotechnical properties of fine sand. *Geomech. Geoenviron.* **2013**, *8*, 86–96. [[CrossRef](#)]
7. Lim, S.K.; Hussin, M.W.; Zakaria, F.; Ling, T.C. GGBFS as potential filler in polyester grout: Flexural and toughness. *Constr. Build. Mater.* **2009**, *23*, 2007–2015. [[CrossRef](#)]
8. Chhun, K.T.; Lee, S.H.; Keo, S.A.; Yune, C.Y. Effect of Acrylate-Cement Grout on the Unconfined Compressive Strength of Silty Sand. *KSCE J. Civ. Eng.* **2019**, *23*, 2495–2502. [[CrossRef](#)]
9. Persoff, P.; Apps, J.; Moridis, G.; Whang, J.M. Effect of dilution and contaminants on sand grouted with colloidal silica. *J. Geotech. Geoenviron. Eng.* **1999**, *125*, 461–469. [[CrossRef](#)]
10. Ciardi, G.; Vannucchi, G.; Madiati, C. Effects of Colloidal Silica Grouting on Geotechnical Properties of Liquefiable Soils: A Review. *Geotechnics* **2021**, *1*, 460–491. [[CrossRef](#)]
11. Vranna, A.; Tika, T. The Mechanical Response of a Silty Sand Stabilized with Colloidal Silica. *Geotechnics* **2021**, *1*, 243–259. [[CrossRef](#)]
12. Anagnostopoulos, C.A.; Dimitriadi, M. Study on high performance polymer-modified cement grouts. *CivilEng* **2021**, *2*, 134–157. [[CrossRef](#)]
13. Xia, Q.; Wen, J.; Tang, X.; Zhu, Y.; Xu, Z.; Du, Z.; Liu, X. Optimal preparation and degradation characterization of repair mortar containing waterborne epoxy resin emulsions. *Constr. Build. Mater.* **2021**, *298*, 123839. [[CrossRef](#)]
14. Issa, S.A.; Debs, P. Experimental study of epoxy repairing of cracks and concrete. *Constr. Build. Mater.* **2007**, *21*, 157–163. [[CrossRef](#)]
15. Wu, L.; Hoa, S.V.; Ton-That, M. Effects of water on the curing and properties of epoxy adhesive used for bonding FRP composite sheet to concrete. *J. Appl. Polym. Sci.* **2003**, *92*, 2261–2268. [[CrossRef](#)]
16. Anagnostopoulos, C.A.; Hadjispyrou, S. Laboratory study of an epoxy resin grouted sand. *Proc. Inst. Civ. Eng. Ground Improv.* **2004**, *8*, 39–45. [[CrossRef](#)]
17. Al-Khanbashi, A.; Abdala, S.W. Evaluation of three waterborne polymers as stabilizers for sandy soil. *Geotech. Geol. Eng.* **2006**, *24*, 1603–1625. [[CrossRef](#)]
18. Anagnostopoulos, C.A.; Kandiliotis, P.; Lola, M.; Karavatos, S. Improving properties of sand using epoxy resin and electrokinetics. *Geotech. Geol. Eng.* **2014**, *32*, 859–872. [[CrossRef](#)]
19. Anagnostopoulos, C.A.; Sapidis, G. Mechanical behaviour of epoxy resin-grouted sand under monotonic or cyclic loading. *Geotech. Lett.* **2017**, *7*, 298–303. [[CrossRef](#)]
20. Anagnostopoulos, C.A. Strength properties of an epoxy resin and cement-stabilized silty clay soil. *Appl. Clay Sci.* **2015**, *114*, 517–529. [[CrossRef](#)]
21. Ghasemzadeh, H.; Mehrpajouh, A.; Pishvaei, M. Laboratory analyses of kaolinite stabilized by vinyl polymers with different monomer types. *Eng. Geol.* **2021**, *280*, 105938. [[CrossRef](#)]
22. Halabian, A.M.; Shakibzadeh, A.; Rowshan, Z.M.A. The static and dynamic behavior of sands grouted with amino-based resin. *Proc. Inst. Civ. Eng. Ground Improv.* **2018**, *171*, 21–37. [[CrossRef](#)]

23. Anagnostopoulos, C.A.; Dimitriadi, M.; Konstantinidis, D. Static and cyclic behavior of epoxy resin and bentonite-grouted sands. *Transp. Geotech.* **2022**, *33*, 100725. [[CrossRef](#)]
24. *ASTM D 4320*; Standard Practice for Laboratory Preparation of Chemically Grouted Soil Specimens for Obtaining Engineering Parameters. ASTM International: West Conshohocken, PA, USA, 2009.
25. Anagnostopoulos, C.A. Effect of different superplasticisers on the physical and mechanical properties of cement grouts. *Constr. Build. Mater.* **2014**, *50*, 162–168. [[CrossRef](#)]
26. *ASTM D 4219*; Standard Test Method for Unconfined Compressive Strength Index of Chemical-Grouted Soils. ASTM International: West Conshohocken, PA, USA, 2002.
27. Neithalath, N.; Weiss, J.; Olek, J. Characterizing enhanced porosity concrete using electrical impedance to predict acoustic and hydraulic performance. *Cem. Concr. Res.* **2006**, *36*, 2074–2085. [[CrossRef](#)]
28. *ASTM D 5084*; Standard Test Methods for Measurement of Hydraulic Conductivity of Saturated Porous Materials Using a Flexible Wall Permeameter. ASTM International: West Conshohocken, PA, USA, 2003.
29. Powers, D.A. *Interaction of Water with Epoxy*; Sandia Report, SAND2009-4405; U.S. Department of Energy's National Nuclear Security Administration: Albuquerque, NW, USA, 2009.
30. Consoli, N.C.; Foppa, D.; Festugato, L.; Heineck, K.S. Key parameters for strength control of artificially cemented soils. *J. Geotech. Geoenvironmental Eng.* **2007**, *133*, 197–205. [[CrossRef](#)]
31. Markou, I.; Droudakis, A. Factors affecting engineering properties of microfine cement grouted sands. *Geotech. Geol. Eng.* **2013**, *31*, 1041–1058. [[CrossRef](#)]
32. Avci, E.; Mollamahmutoglu, M. UCS properties of superfine cement-grouted sand. *J. Mater. Civ. Eng.* **2016**, *28*, 06016015. [[CrossRef](#)]
33. Doherty, P.; Spagnoli, G.; Doherty, M. Laboratory investigations to assess the feasibility of employing a novel mixed-in-place offshore pile in calcareous deposits. *Ships Offshore Struct.* **2020**, *15*, 29–38. [[CrossRef](#)]
34. Jafarian, Y.; Javdanian, H. Dynamic Properties of Calcareous Sand from the Persian Gulf in Comparison with Siliceous Sands Database. *Int. J. Civ. Eng.* **2020**, *18*, 245–249. [[CrossRef](#)]
35. Cui, M.J.; Zheng, J.J.; Chu, J.; Wu, C.C.; Lai, H.J. Bio-mediated calcium carbonate precipitation and its effect on the shear behaviour of calcareous sand. *Acta Geotech.* **2021**, *16*, 1377–1389. [[CrossRef](#)]
36. Hamidi, S.; Marandi, S.M. Clay concrete and effect of clay minerals types on stabilized soft clay soils by epoxy resin. *Appl. Clay Sci.* **2018**, *151*, 92–101. [[CrossRef](#)]
37. Ata, A.; Vipulanandan, C. Factors affecting mechanical and creep properties of silicate-grouted sands. *Geotech. Geol. Eng.* **1999**, *125*, 868–876. [[CrossRef](#)]
38. Ribay, E.D.; Maigre, I.D.; Cabrillac, R.; Gouvenot, D. Influence of grouts on unconfined creep behaviour of grouted Fontainebleau sand: Experimental and primary creep modeling. *Proc. Inst. Civ. Eng. Ground Improv.* **2002**, *6*, 23–37. [[CrossRef](#)]
39. Ribay, E.; Maigre, I.; Cabrillac, R.; Gouvenot, D. Comparison of creep behavior and fatigue behavior of grouted sand. *Soils Found.* **2007**, *47*, 185–194. [[CrossRef](#)]
40. Chen, Z.J.; Feng, W.Q.; Yin, J.H. A new simplified method for calculating short-term and long-term consolidation settlements of multi-layered soils considering creep limit. *Comput. Geotech.* **2021**, *138*, 104324. [[CrossRef](#)]
41. Mollamahmutoglu, M.; Avci, E.; Devci, E. Strength and permeability properties of sodium silicate-glyoxal-stabilized silt and fine sand. *Q. J. Eng. Geol. Hydrogeol.* **2022**, *55*, qjgh2021-115. [[CrossRef](#)]

Disclaimer/Publisher's Note: The statements, opinions and data contained in all publications are solely those of the individual author(s) and contributor(s) and not of MDPI and/or the editor(s). MDPI and/or the editor(s) disclaim responsibility for any injury to people or property resulting from any ideas, methods, instructions or products referred to in the content.